12th Brazilian Congress of Manufacturing Engineering
May 10th-12th, 2023, Brasilia, DF, Brazil

# BARKHAUSEN NOISE CORRELATION WITH SURFACE RESIDUAL STRESS ON MARAGING STEEL WHEN COMBINING ADDITIVE MANUFACTURING, AGING, AND MILLING

**Amanda Rossi de Oliveira**
Centro de Engenharia, Modelagem e Ciências Sociais Aplicadas, Universidade Federal do ABC, Santo André, Brazil.
Av. dos Estados, 5001, 09210-580, Santo André, São Paulo, Brazil
a.rossi@ufabc.edu.br

**Vitor Furlan de Oliveira**
Universidade de São Paulo, Escola Politécnica, São Paulo, Brazil
Av. Prof. Luciano Gualberto, 380, 05508-010, Butantã, São Paulo, Brazil
vitor.furlan@usp.br

**Julio Carlos Teixeira**
Centro de Engenharia, Modelagem e Ciências Sociais Aplicadas, Universidade Federal do ABC, Santo André, Brazil.
Av. dos Estados, 5001, 09210-580, Santo André, São Paulo, Brazil
juliocarlos.teixeira@ufabc.edu.br

**Sydney Ferreira Santos**
Centro de Engenharia, Modelagem e Ciências Sociais Aplicadas, Universidade Federal do ABC, Santo André, Brazil.
Av. dos Estados, 5001, 09210-580, Santo André, São Paulo, Brazil
sydney.ferreira@ufabc.edu.br

**Erik Gustavo Del Conte**
Centro de Engenharia, Modelagem e Ciências Sociais Aplicadas, Universidade Federal do ABC, Santo André, Brazil.
Av. dos Estados, 5001, 09210-580, Santo André, São Paulo, Brazil
erik.conte@ufabc.edu.br

***Abstract.*** *Laser Powder Bed Fusion (LPBF) of metallic components promotes tailored properties advantages in contrast to conventional subtractive technologies, mainly due to the numerous processing parameters that can be managed. On the other hand, this freedom can lead to repeatability issues for the additive technique, requiring the definition of quality inspection strategies sensitive to processing changes. Materials like maraging steel require some post-processing upon LPBF to achieve the properties and surface conditions necessary for specific applications, for example, injection molds. Thus, nondestructive inspection methods sensitive to the stress behavior, such as the Magnetic Barkhausen Noise (MBN), may benefit the residual stress evaluation in components manufactured with a combination of LPBF and other operations. The MBN phenomenon is observed as pulses induced by discontinuities in domain walls motion in ferromagnetic materials during the magnetization process when subjected to a time-varying external magnetic field. So, this study investigated possible correlations between the MBN and the surface residual stress when combining LPBF, aging treatment (480 ºC for 3 hours), and milling with cutting speed variations (150 m/min and 250 m/min). MBN had its signal collected along the feed direction for signal energy determination to correlate with surface residual stress values assessed with X-ray diffraction. It was possible to observe different Pearson correlation coefficients between the surface residual stress, MBN, and processing parameters. Thus, it was possible to define a linear model to support the surface residual stress prediction based on the features that showed statistical significance for this property within a 0.95 confidence interval, including the MBN energy. Finally, the obtained findings were compared with previous works that explored the MBN inspection focused on the LPBF technology. As a result, the present study contributes to understanding whether the MBN use is feasible for inspecting maraging steel components manufactured with combined processing of LPBF and milling or not.*

***Keywords:*** *laser powder bed fusion; milling; residual stress; barkhausen noise; nondestructive inspection.*

## 1. INTRODUCTION

Engineering components fabrication is facing the evolution of a revolutionary technology called Additive Manufacturing (AM). Unlike the conventional subtractive processes, the new technique takes advantage of a bottom-up strategy to obtain freeform bulk materials. So, using an iterative approach for layers construction, the AM technology

improves manufacturing flexibility from home decoration artifacts to prostheses and structural parts for engineering, considering the wide range of compatible materials.

Regarding the fabrication of metallic components, one of the available AM techniques is Laser Powder Bed Fusion (LPBF). In this approach, material powder particles are fused by a laser scanning system, giving rise to a component previously defined in a computational model (ASTM International, 2021). Flexibility gains with the LPBF technology favor the achievement of high-complex shapes with lesser materials waste than conventional subtractive techniques; however, it must bear in mind that such versatility can affect products' quality management (Guddati *et al.*, 2019). Guo et al. (2022) extensively reviewed many LPBF parameters that can affect the mechanical performance of maraging components. Regarding residual stress, a critical property for structural applications (Noyan and Cohen, 1986; Mercelis and Kruth, 2006), parameters capable of changing the thermal gradients during manufacturing, like laser power or scan strategy, were found to contribute to the final residual stress (Guo *et al.*, 2022). So, an issue to be addressed in the quality inspection of LPBF manufactured parts is the establishment of measurement techniques sensitive to processing parameters tuning.

Using nondestructive evaluation (NDE) is of great interest for additive manufacturing advancements, considering the necessity to ensure high-quality standard products without damaging the manufactured parts (Mandache, 2019; Charalampous, Kostavelis and Tzovaras, 2020). Moreover, the NDE approach can be a valuable tool for evaluating products obtained with AM coupled with some common post-processing operations (Mandache, 2019). For maraging steel, aging treatment is commonly applied to enhance tensile strength and hardness performance because of an intermetallic precipitation mechanism (A. R. Oliveira *et al.*, 2021). Furthermore, milling can be used for surface finishing after LPBF (Fortunato *et al.*, 2018; Bai *et al.*, 2021). Thus, selecting a good NDE technique should also consider the different stages involved in component fabrication to provide a comparative analysis within the fabrication chain.

The Magnetic Barkhausen Noise (MBN) phenomenon is observed as pulses induced by discontinuities in domain walls motion in ferromagnetic materials during the magnetization using an external magnetic field that varies in time. How elastic stresses in a material affect the magnetic domain walls motion, known as magnetoelasticity, can change the MBN signal intensities, providing a potential tool for surface residual stress inspection (Deveci and Stresstech, 2017). Despite the successful applications of the MBN for inspecting ferromagnetic materials produced by conventional manufacturing routes (Del Conte *et al.*, 2016; Le Manh, Pérez Benitez and Alberteris, 2020), the implementation of this type of NDE strategy requires further investigation when mixing manufacturing technologies. Thus, this study aimed to analyze the feasibility of using metrics extracted from the MBN signal to inspect the surface residual stress upon LPBF, aging (480 ºC for 3 hours), and milling with cutting speed variations (150 m/min and 250 m/min). This way, experimental results were subjected to statistical analysis for correlation investigations. Finally, a model could be proposed for surface residual stress based on the manufacturing parameters and the MBN energy.

## 2. MATERIALS AND METHODS

### 2.1 Manufacturing: LPBF, aging heat treatment, and milling

The 32x32x10 mm cuboid samples used for the experiments were manufactured using the EOS M280 system. Maraging steel gas atomized particles supplied by Carpenter Additive/LPW (Cheshire, United Kingdom) were used as the raw material for LPBF, considering the chemical composition shown in Tab. 1. The additive manufacturing used a zig-zag scan pattern with 67º rotation between adjacent layers. The laser of 170 W power defined layers with 0.02 mm thickness. These parameters are within the processing window capable of fabricating parts with relative densities even higher than 99%, according to the defined incident energy density (Mutua *et al.*, 2018; Oliveira, Jardini and Del Conte, 2020).

Table 1. Maraging powder chemical compositions according to the supplier (Carpenter Additive, 2019).

| **Al** | **Ti** | **Si** | S | P | **O** | **Ni** | **N** | **Mo** | **Mn** | **Cr** | **Co** | **C** | **Fe** |
|---|---|---|---|---|---|---|---|---|---|---|---|---|---|
| **0.1** | **0.9** | **0.03** | **0.002** | **0.005** | **0.03** | **18.11** | **<0.01** | **4.9** | **0.02** | **0.03** | **9.02** | **0.02** | **Balance** |

After LPBF, half of the manufactured samples were exposed to a typical aging heat treatment for maraging steel (Conde *et al.*, 2019). In this context, the performed aging used a muffle furnace to maintain the 480 ºC temperature for 3 hours, and the final air cooling process occurred under room conditions. Samples that remained as built by LPBF were named 'AB,' and the heat treated ones were named 'HT'. Finally, both manufactured batches had their 32x32 mm surfaces machined using the 3-axis CNC machining center Mi 136 II (Santa Barbara D'Oeste, Brazil). Fixing the depth of cut ($a_p$) in 0.1 mm and the feed rate ($f_z$) of 0.02 mm/tooth, a surface leveling was performed on each surface, and then one finishing operation was executed with varying cutting speeds ($v_c$) of 150 m/min and 250 m/min. All operations used two flutes cemented carbide end mill tools with a diameter of 6 mm (Dormer, Šumperk, Czech Republic). The experiments were performed according to the full factorial design of experiments (DoE) with the processing parameters detailed in Tab. 2. Final surfaces were observed with optical microscopy using the Zeiss Scope A1 AxioCam microscope (Jena, Germany).

Table 2. Post-processing control variables for each studied condition.

| Experimental condition | Direct aging (480 ºC for 3h) | Milling cutting speed [m/min] |
|---|---|---|
| #AB_150 | No | 150 |
| #AB_250 | No | 250 |
| #HT_150 | Yes | 150 |
| #HT_250 | Yes | 250 |

## 2.2 MBN and residual stress evaluation plans

The MBN signal collection involves the application of an external magnetic field combined with an excitation and detection probe and acquisition equipment to capture the sample responses. Thus, the external magnetic field was generated with the Rollscan 250 Stresstech device (Vaajakoski, Finland) using an excitation voltage of 6 V, a 100 Hz frequency, and a 55 $mm^2$ ferromagnetic probe (Fig. 1). MBN signal was acquired along with the milling feed direction using a NI USB-6351 (National Instruments, Texas, United States) data acquisition board under a 250 kHz sampling frequency. All these parameters followed previous studies (A. R. de Oliveira *et al.*, 2021; de Oliveira *et al.*, 2021).

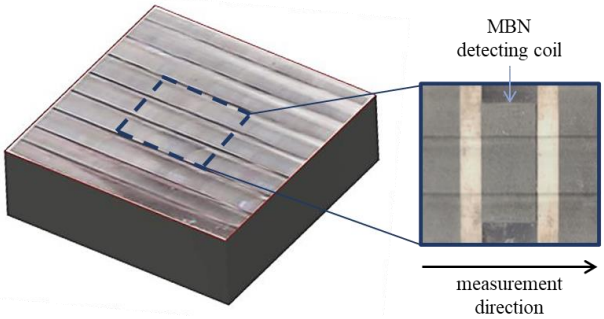


Figure 1. Region of surface residual stress and MBN signal measurements.

The measurements were stored in a computer for signal analysis with the NI DAQExpress software. Also, signals were used for MBN energy determination based on numerical integrations executed with MATLAB, according to Eq. 2, where $V^2$ referred to the squared measured signal pulses and n represented the 25000 evaluated pulses per second (Krause, Clapham and Atherton, 1994; Del Conte *et al.*, 2016).

$$MBN\ energy = \frac{1}{n}\int_{1}^{n} V^2\, dt \tag{1}$$

Surface residual stress measurements, along with the milling feed direction, were obtained with the X-ray diffraction (XRD) technique in the Stresstech G2R machine (Rennerod, Germany). Measured using a Cr-Kα tube (λ = 0.2291 nm) with an incidence angle of 0º and a diffraction angle of 156.4°, the residual stress values were provided directly by the Xtronic machine software, considering the cross-correlation peak search within the experimental conditions of 7.5 mA current and 25 kV voltage under a 9 s exposure. Each analyzed condition had three replicates for mean property determination. Surface residual stress results were previously published (Oliveira and Del Conte, 2021).

To sum up, an overall of the experimental activities that generated data for the study is shown in Figure 2.

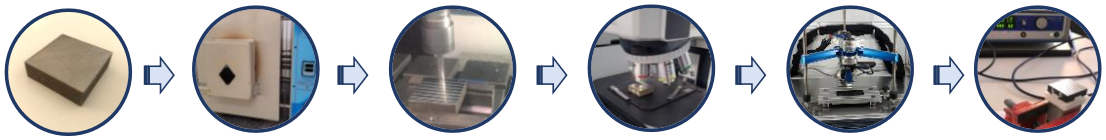


Figure 2. Experimental activities performed in the study.

Statistical tools were used to validate experimental results of surface residual stress and MBN energy. Firstly, the Pearson correlation coefficient (r), a metric commonly applied for identifying the linear relationship between variables (Belfiore, 2015), was used for further understanding how the surface residual stress could be quantitatively explained by the MBN energy, according to the manufacturing conditions. Then, an Analysis of Variance (ANOVA) was performed to identify the manufacturing process that effectively affected the surface residual stress within a 95% confidence interval. ANOVA supported the linear fitting of this property based on the manufacturing and associated MBN energy. The statistical analyses were conducted with the Action Stat Pro software.

## 3. RESULTS AND DISCUSSION

### 3.1 MBN energy for different processing conditions

MBN signals collected for each manufacturing condition are shown in Fig. 3. It is possible to observe differences among signal intensities depending on the manufacturing condition. Additionally, peak shapes changed mainly between the as built and aged samples. In this sense, after milling, the MBN signal found for the as built samples has higher maximum peak amplitudes than the aged samples. On the other hand, the width of the peaks did not significantly vary when switching the evaluated manufacturing parameters. Thus, it is essential to compare the observed behavior with the surface residual stress results to understand the main sources of changes in the MBN signal based on the material attributes.

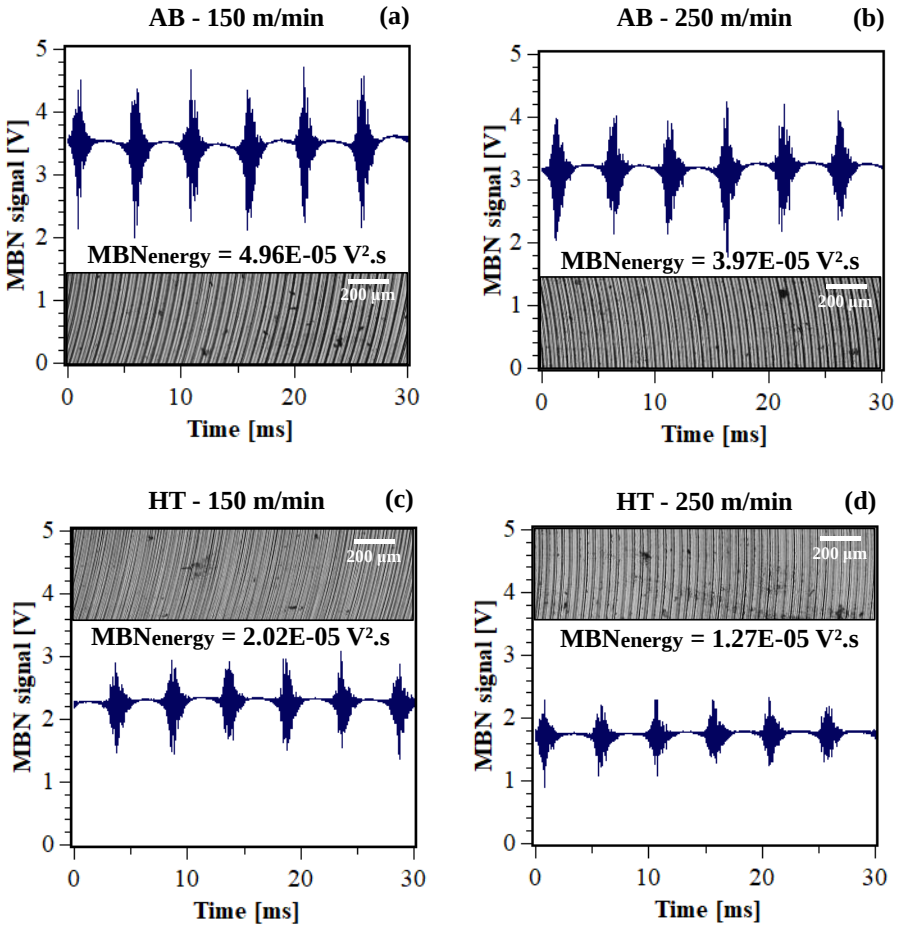


Figure 3. MBN signals collected for AB samples milled with (a) $v_c$ = 150 m/min and (b) $v_c$ = 250 m/min, and HT samples milled with (c) $v_c$ = 150 m/min and (d) $v_c$ = 250 m/min. The insets show the surface finishing observed for each manufacturing condition.

MBN energy metrics were extracted from the collected signals (Eq. 1) and shown in Fig. 3. Additionally, these results were plotted against the average surface residual stress previously found for each manufacturing condition (Oliveira and Del Conte, 2021), resulting in the relation shown in Fig. 4. Considering a linear fitting between both variables with a coefficient of determination ($R^2$) of 0.94, the surface residual stress could be statistically well explained by the MBN energy. Increased compressive surface residual stresses could be found at the same time as reduced MBN energies and signal peak amplitudes (Figs. 3 and 4). These findings can be attributed to a positive magnetoelasticity of maraging steel, as discussed in the literature, which corresponds to a direct relationship between MBN intensities and tensile stresses and an indirect relation between MBN and compressive stresses (Deveci and Stresstech, 2017; A. R. de Oliveira *et al.*, 2021; de Oliveira *et al.*, 2021).

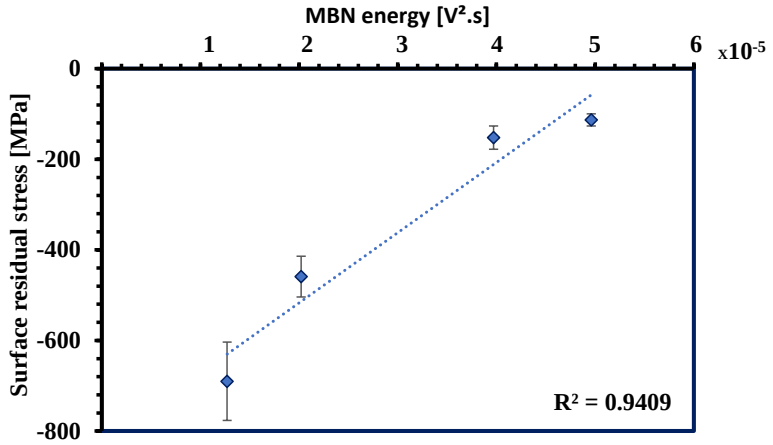


Figure 4. Average surface residual stress and MBN energy for each manufacturing condition.

Considering the potential of MBN energy to explain the studied surface residual stress (Fig. 4), the Pearson correlation coefficient (r) associated with the linear correlation observed for all the surface residual stress and MBN energy results was determined. The obtained result was stated as "Full data" in Tab. 3. Also, correlations were individually analyzed for each post-processing, according to the treatment level (as built or aged) and the cutting speed used in milling (150 or 250 m/min). The obtained metrics are shown in Tab. 3.

Table 3. Pearson correlation coefficients between the MBN energy and residual stress for different parameters.

| **Statistical metrics** | **Full data** | **Treatment** | | **Milling cutting speed** | |
|---|---|---|---|---|---|
| | | **As built** | **Aged** | **150 m/min** | **250 m/min** |
| Pearson coefficient (r) | 0.96 | 0.85 | 0.82 | 0.99 | 0.97 |
| p-value | 1.32E-06 | 0.030 | 0.046 | 5.93E-05 | 0.001 |

A very strong positive Pearson correlation coefficient was found for all the MBN energy and surface residual stress results, considering the value of 0.96. This finding indicates the feasibility of using the MBN energy to inspect the surface residual stress of maraging steel components manufactured by LPBF and post-processed with aging (480 ºC for 3 hours) and milling.

To compare the relations between the two properties upon milling, focused on the levels of treatment and cutting speed, additional Pearson coefficients were determined (Tab. 3). So, there are just slight differences between r when changing the treatment levels or milling cutting speeds. Considering that all r coefficients showed strong or very strong positive correlations between MBN energy and the surface residual stress, there is no statistical counterpoint to proposing a fitting model for inspecting the residual stress based on the studied manufacturing parameters.

### 3.2 Residual stress modeling with MBN energy

Obtaining an adequate model for surface residual stress inspection based on the processing parameters can improve the quality management of the LPBF process. So, the Analysis of Variance allowed the validation of which factors influence the surface residual stress within a 0.95 confidence interval, as shown in Tab. 4. Although the heat treatment showed the main influence on surface residual stress, all evaluated factors showed statistical effects on the stress response, as evidenced by the p-values < 0.05. Also, these analyses agreed with the correlation evaluations performed in Section 3.1.

Table 4. ANOVA for surface residual stress regression.

| **Factors** | **F statistics** | **p-value** |
|---|---|---|
| Treatment, T | 3700.83 | 4.37E-07 |
| Cutting speed, $v_c$ | 310.24 | 6.10E-05 |
| MBN energy | 63.76 | 0.0013 |
| T* $v_c$ | 90.27 | 0.0007 |
| T* MBN energy | 31.34 | 0.0050 |
| $v_c$ *MBN energy | 37.83 | 0.0035 |
| T* $v_c$ *MBN energy | 53.36 | 0.0019 |

In this context, a linear fitting model could be proposed for the surface residual stress prediction according to the studied post-processing parameters, as shown in Eq. 2, where T assumes 0 for as built samples and 1 for aged samples, and $v_c$ assumes 0 for the milling cutting speed of 150 m/min and the value 1 for 250 m/min. MBN energy is still a continuous variable in the model because there were no level attributions to this parameter during the Design of Experiments implementation. The model adjusted coefficient of determination ($R^2adj$) is 0.997, reinforcing the curve adequation to model the residual stress data.

$$RS_{surface} = -776 - 594*T - 252*v_c + 13346569*MBNenergy + 1828*T*v_c + 31235164*T*MBNenergy + 8731456*v_c*MBNenergy - 123942125*T*v_c*MBNenergy \quad (2)$$

Figure 5 compares the experimental and fitted average surface residual stress using the proposed model (Eq. 2). The error bars define the standard deviation within the three replicates performed according to the DOE. The model achieved relative errors lower than 4.5%. So, its performance corroborated the great accuracy expressed by the $R^2adj$, providing a helpful tool for the nondestructive evaluation of surface residual stress of LPBF manufactured components upon milling.

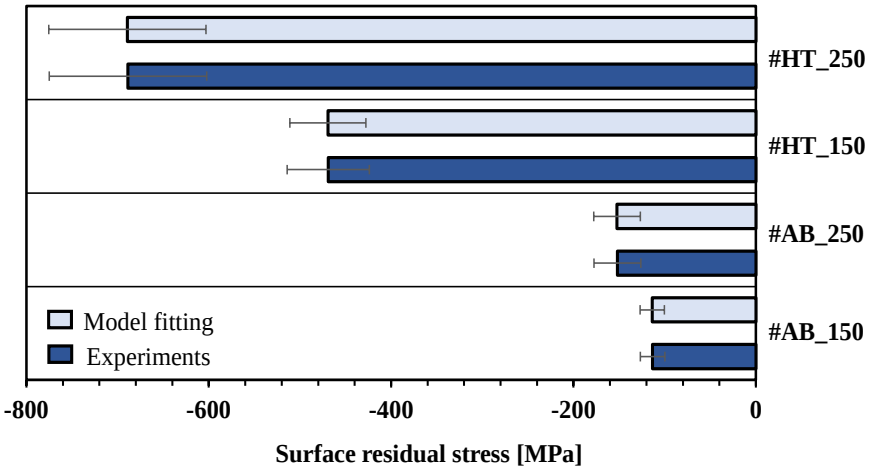


Figure 5. Comparison of experimental and fitted surface residual stress according to processing parameters.

### 3.3 Comparison with the literature

Machining operations tend to define surface residual stress with compressive behavior, even though cutting parameters can influence the obtained results (Guo *et al.*, 2017; Acevedo *et al.*, 2020). This phenomenon is related to plastic deformations or/and phase transformations induced by milling on the material surface and subsurface (Brinksmeier *et al.*, 2008). Additionally, differences between the as built and aged mechanical properties were expected to change the cutting mechanism during milling (Oliveira and Del Conte, 2021). As a result, distinct correlations between MBN signal features and the surface residual stress might be found compared to those observed for samples exclusively manufactured by LPBF and aged. So, the following paragraphs will compare the obtained results with previous studies to determine whether the MBN would effectively represent the residual stress.

Differently from the literature findings (de Oliveira *et al.*, 2021), which showed just a moderate correlation of 0.63 between the surface residual stress and MBN energy for the aging treated samples before milling, in the present study, it was possible to obtain a high correlation (0.82) between these features upon combined aging and milling post-processing (Tab. 3). These observations may be attributed to the higher differences found for the surface residual stress depending on the milling cutting speed for the aged samples, which might facilitate the MBN energy sensitivity to respond to this material property.

Regarding the as built samples, similar correlation coefficients were observed between the MBN energy and surface residual stress independently of the milling operation (de Oliveira *et al.*, 2021). When exclusively manufactured by LPBF, the literature showed a correlation of 0.86 (de Oliveira *et al.*, 2021). Likewise, in the present study, a correlation of 0.85 was found for as built samples upon milling (Tab. 3). Thus, following the behavior discussed for the aged samples, lesser differences in the magnitude of surface residual stress may contribute to the matching correlations.

It is possible to discuss potential applications of the MBN measurement to inspect the surface residual stress. In addition to the proposed modeling that can provide predictions for the residual stress according to key fabrication parameters, an online monitoring system can be defined to improve further inspection agility (Del Conte *et al.*, 2016). In a more complex way, control systems might be projected to use the MBN measurements for tuning the manufacturing parameters in real time, depending on the final product requirements. Finally, the studied approach expanded the insights

about using the MBN nondestructive inspection for maraging steel components manufactured by LPBF and post-processed with aging treatment and milling.

## 4. CONCLUSIONS

The MBN energy extracted from the collected signals was found to highly correlate (r = 0.96) with the experimental measurements of surface residual stress for maraging samples upon LPBF, aging (480 ºC for 3 hours), and milling with cutting speed variations (150 m/min and 250 m/min). Also, ANOVA evidenced that all varied processing parameters could influence the final surface residual stresses. So, a fitting model could be proposed for surface residual stress based on the manufacturing parameters and the MBN energy, which could reach an accurate performance with $R^2adj = 0.997$ and relative errors lower than 5% from the experimental results. Hence, the study provides a helpful strategy for nondestructive evaluating a critical property for maraging steel applications, also highlighting a potential NDE solution to be investigated for other ferromagnetic materials manufactured with LPBF and finished with milling.

## 5. ACKNOWLEDGEMENTS

The authors thank Dr. André Luiz Jardini from the National Institute of Biofabrication (INCT-BIOFABRIS) and Eng. Alisson D. C. Nizes from Thyssenkrupp Brasil (Division Springs and Stabilizers). This study was financed by the São Paulo Research Foundation (FAPESP) under grant numbers #2018/11282-0, #2021/00553-6, and #2021/09890-5. This study was financed in part by the Coordenação de Aperfeiçoamento de Pessoal de Nível Superior - Brasil (CAPES) - Finance Code 001.

## 6. REFERENCES

Acevedo, R., Sedlak P., Kolman, R., and Fredel M., 2020. Residual stress analysis of additive manufacturing of metallic parts using ultrasonic waves: State of the art review. *Journal of Materials Research and Technology*, Vol. 9, n. 4, pp. 9457–9477.

ASTM International, 2021. *ISO/ASTM 52900:2021 (en) Additive manufacturing — General principles — Fundamentals and vocabulary*. Pennsylvania.

Bai, Y. et al., 2021. Microstructure and machinability of selective laser melted high-strength maraging steel with heat treatment. *Journal of Materials Processing Technology*, Vol. 288, pp. 1–18.

Belfiore, P., 2015. Estatística aplicada a administração, contabilidade e economia com Excel e SPSS. 1st ed. Editora GEN LTC, Rio de Janeiro.

Brinksmeier, E. et al., 2008. Residual Stresses — Measurement and Causes in Machining Processes. *CIRP Annals*, Vol. 31, pp. 491–510.

Carpenter Additive, 2019. *Test Certificate*.

Charalampous, P., Kostavelis, I. and Tzovaras, D., 2020. Nondestructive quality control methods in additive manufacturing: a survey. *Rapid Prototyping Journal*, Vol. 26, pp. 777–790.

Conde, F.F. et al., 2019. Effect of thermal cycling and aging stages on the microstructure and bending strength of a selective laser melted 300-grade maraging steel. *Materials Science and Engineering A*, Vol. 758, pp. 192–201.

Del Conte, E.G. et al., 2016. Barkhausen Noise Analysis as an Alternative Method to Online Monitoring of Milling Surfaces. IEEE Transactions on Magnetics, Vol. 52.

Deveci, M. and Stresstech, 2017. Stresstech Bulletin 2: The Properties of Barkhausen Noise. 25 Jun. 2021. <https://www.stresstech.com/stresstech-bulletin-2-the-properities-of-barkhausen-noise/>.

Fortunato, A. et al., 2018. Milling of maraging steel components produced by selective laser melting. *The International Journal of Advanced Manufacturing Technology*, Vol. 94, pp. 1895–1902.

Guddati, S. et al., 2019. Recent advancements in additive manufacturing technologies for porous material applications. *The International Journal of Advanced Manufacturing Technology*, Vol. 105, pp. 193–215.

Guo, L. et al., 2022. Additive manufacturing of 18% nickel maraging steels: Defect, structure and mechanical properties: A review. *Journal of Materials Science & Technology*, Vol. 120, pp. 227–252.

Guo, P. et al., 2017. Study on microstructure, mechanical properties and machinability of efficiently additive manufactured AISI 316L stainless steel by high-power direct laser deposition. *Journal of Materials Processing Technology*, Vol. 240, pp. 12–22.

Krause, T.W., Clapham L., and Atherton D.L., 1994. Characterization of the magnetic easy axis in pipeline steel using magnetic Barkhausen noise. *Journal of Applied Physics*, Vol. 75, pp. 7983–7988.

Mandache, C., 2019. Overview of nondestructive evaluation techniques for metal-based additive manufacturing. *Materials Science and Technology*, Vol. 35, pp. 1007–1015.

Le Manh, T., Pérez Benitez, J.A. and Alberteris, M., 2020. Future trend and applications of Barkhausen noise in *Barkhausen Noise for Nondestructive Testing and Materials Characterization in Low Carbon Steels.* Elsevier, pp. 239–253.

Mercelis, P. and Kruth, J.P., 2006. Residual stresses in selective laser sintering and selective laser melting. *Rapid Prototyping Journal*, Vol. 12, pp. 254–265.

Mutua, J. et al., 2018. Optimization of selective laser melting parameters and influence of post heat treatment on microstructure and mechanical properties of maraging steel. *Materials and Design*, Vol. 139, pp. 486–497.

Noyan, I.C. and Cohen, J.B., 1986. *Residual Stress*: Measurement by Diffraction and Interpretation, Journal of Chemical Information and Modeling. Springer Science+Business Media, New York.

Oliveira, A.R. et al., 2021. Investigation of Building Orientation and Aging on Strength–Stiffness Performance of Additively Manufactured Maraging Steel. *Journal of Materials Engineering and Performance*, Vol. 30, pp. 1479–1489.

Oliveira, A.R. et al., 2022. Barkhausen Noise monitoring of microstructure and surface residual stress in maraging steel manufactured by Powder Bed Fusion and aging. The International Journal of Advanced Manufacturing Technology, Vol. 119, pp.1835–1852.

Oliveira, A.R. et al., 2021. Investigation of the build orientation effect on magnetic properties and Barkhausen Noise of additively manufactured maraging steel 300. *Additive Manufacturing*, Vol. 38.

Oliveira, A.R., and Del Conte, E.G., 2021. Concurrent improvement of surface roughness and residual stress of as-built and aged additively manufactured maraging steel post-processed by milling. *The International Journal of Advanced Manufacturing Technology*, 116, pp. 2309–2323.

Oliveira, A.R., Jardini, A.L., and Del Conte, E.G., 2020. Effects of cutting parameters on roughness and residual stress of maraging steel specimens produced by additive manufacturing. *The International Journal of Advanced Manufacturing Technology*, Vol. 111, pp. 2449–2459.

## 7. RESPONSIBILITY NOTICE

The authors are the only responsible for the printed material included in this paper.